Synthesis and Characterization of Conducting Poly(3-acetylpyrrole)/Carbon Nanotube Composites

Yuying Zheng,[1] Pan Wang,[2] Baoming Li[1]

[1]*College of Materials Science and Engineering, Fuzhou University, Fuzhou 350108, China*
[2]*College of Chemistry and Chemical Engineering, Fuzhou University, Fuzhou 350108, China*

Received 27 June 2011; accepted 23 October 2011
DOI 10.1002/app.36416
Published online in Wiley Online Library (wileyonlinelibrary.com).

ABSTRACT: Conducting poly(3-acetylpyrrole) (PAPy)/multiwalled carbon nanotubes (MWNTs) composites were synthesized by the *in situ* chemical polymerization of 3-acetylpyrrole (APy) onto MWNTs. The structure and morphology of the PAPy/MWNT composites were characterized by Fourier transform infrared (FTIR) spectroscopy, X-ray diffraction, field emission scanning electron microscopy (FE-SEM), transmission electron microscopy (TEM), and thermogravimetric analysis. The FTIR results indicated that no chemical reaction occurred between the PAPy and MWNTs, and only the MWNTs served as a template for APy polymerization. FE-SEM and TEM suggested that PAPy was only coated on the surface of the carbon nanotubes, and the thickness of the PAPy coating on each nanotube was dependent on the ratio of APy to MWNTs. The standard four-probe method was used to measure the electrical conductivity of the samples at room temperature, and the results show that the MWNTs enhanced the electrical conductivity of the composites compared to PAPy. In addition, the solution stability of the suspension with the PAPy [or polypyrrole (PPy)]/MWNT composites was investigated; this showed that the dispersion of the PAPy/MWNT composites in ethanol solution was much better than that of the PPy/MWNT composites. © 2012 Wiley Periodicals, Inc. J Appl Polym Sci 000: 000–000, 2012

Key words: carbon nanotube; composites; polypyrroles

INTRODUCTION

Carbon nanotubes (CNTs), including single-walled CNTs and multiwalled carbon nanotubes (MWNTs), have attracted a great deal of attention over the last 2 decades because of their exciting electronic, mechanical, thermal, magnetic, and structural properties[1–3] and their promising applications in materials science and medicinal chemistry, such as in energy-storage and energy-conversion devices, nanobiotechnology, sensors, field emission displays, and electronic nanodevices.[4–6]

On the other hand, electrically conducting polymers, such as polypyrrole (PPy), polyaniline, and polythiophene, have received much attention for their unusual electronic and optical properties and have offered several potential applications in solar cells, lightweight batteries, capacitors, sensors, and electronic devices.[7–10] Among the conducting polymers, PPy has superiority for commercial applications because of its unique properties, such as its relative ease of preparation, high electrical conductivity, and environmental stability.[11]

Recently, a great deal of research concerning PPy/CNT composites has been reported;[12] those studies have mainly focused on the structure, morphology, electrical conductivity, and electrochemical analysis of the composites. A variety of methods have been reported on the preparation of composites of PPy and CNTs, including the chemical and electrochemical oxidation methods.[13,14] Sahoo et al.[13] synthesized PPy/MWNT nanocomposites by *in situ* chemical oxidative polymerization. They showed that the electrical conductivity of the nanocomposites was enhanced compared to PPy and MWNTs and was strongly influenced by the feed ratio of pyrrole (Py) to the MWNTs. Karim et al.[14] fabricated PPy/MWNT nanocomposites through an *in situ* γ-radiation-induced chemical polymerization method. They studied the morphology, conductivity, and thermal stability of the composites and showed that the MWNTs were modified by conducting PPy, with various properties enhanced.

It is known that PPy has poor mechanical properties and is insoluble, nonmelting, and not processable; this causes many difficulties in experimenting and processing. To improve the properties, poly(3-acylpyrrole) was synthesized from 3-acylpyrrole with polar substituents (acyl). Poly(3-acylpyrrole)/CNT composites were fabricated by *in situ* chemical

Correspondence to: Y. Zheng (yyzheng@fzu.edu.cn).
Contract grant sponsor: Ministry of Science and Technology of China; contract grant number: 292009GJC40029.

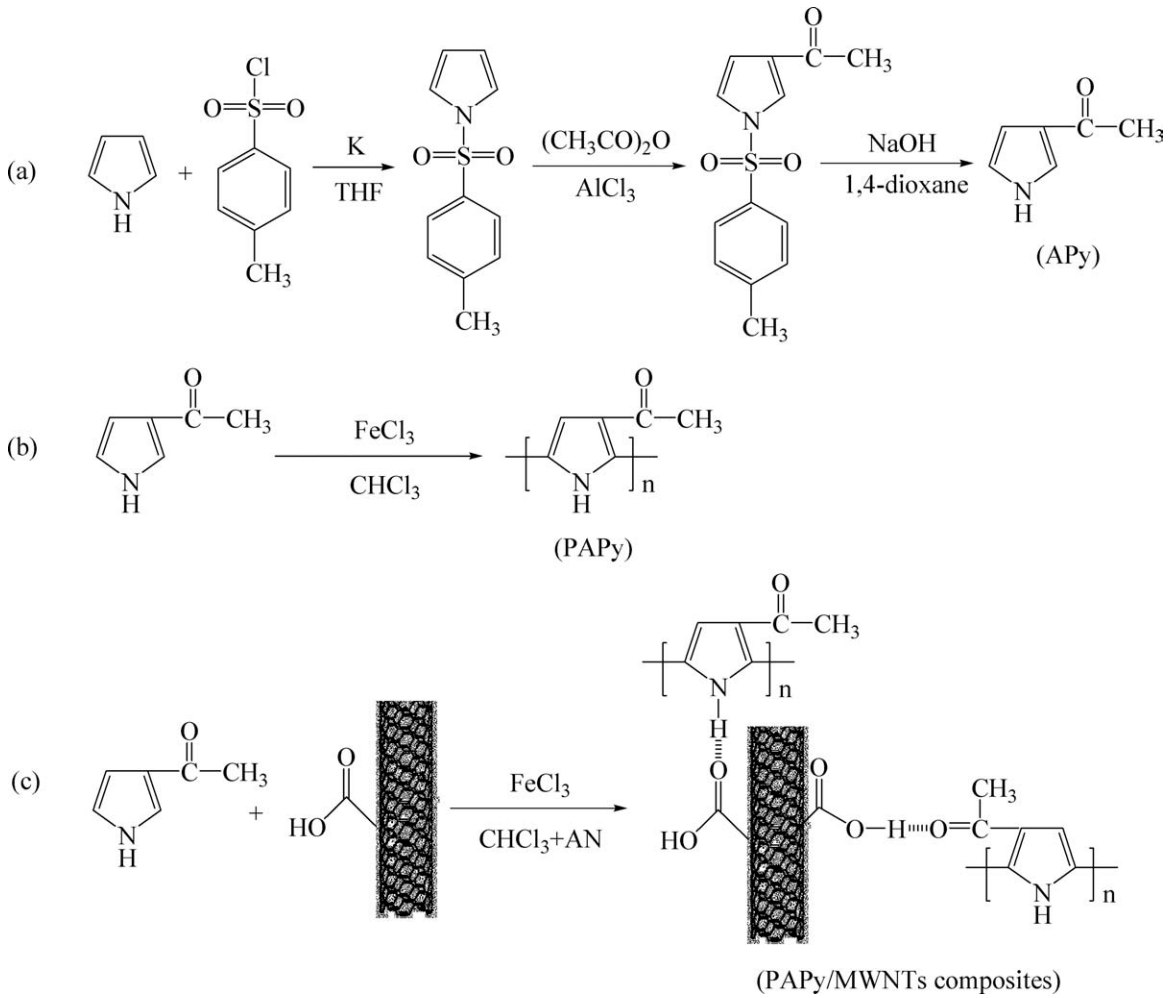

Figure 1 (a) Synthetic route of APy, (b) synthesis of PAPy, and (c) preparation of the PAPy/MWNT composites and possible interactions of hydrogen bonding existing between the PAPy chain and MWNTs (THF = tetrahydrofuran).

polymerization for the first time. Furthermore, we discuss the differences between the properties, such as dispersity and thermal and electrical properties, of poly(3-acylpyrrole)/CNT composites and PPy/CNT composites.

In this article, we report on poly(3-acetylpyrrole) (PAPy)/MWNT composites, which were prepared by an *in situ* chemical polymerization method. The molecular structure and morphology of the resulting composites were characterized, and the physical properties, including the thermal and electrical properties, were investigated. In particular, we discuss the influence of the feed ratio of monomer to CNTs.

EXPERIMENTAL

Materials and preparation of the composites

MWNTs (purity of CNTs > 98%, diameter = 10–30 nm, length = 5–15 μm, specific surface area = 40–300 m^2/g) were purchased from Shenzhen Nanotech Port Co., Ltd. (Shenzhen, China). MWNTs were modified by the following routine: 1.5 g of pristine MWNTs was refluxed in 200 mL of concentrated H_2SO_4/HNO_3 mixed acid (3:1) for 2 h. After air cooling, the mixture was slowly poured into a beaker (1000 mL) with 600 mL of deionized water and then kept overnight. The resulting powder settled to the bottom of the beaker, and the excess liquid was decanted. The remaining liquid and solid particles were separated by centrifugation, washed repeatedly with deionized water, and dried *in vacuo* at 80°C for 24 h. These modified MWNTs (MWNT–COOH, abbreviated to MWNTs) were used in all of the experiments.

3-Acetylpyrrole (APy) was synthesized from Py via a published procedure [Fig. 1(a)].[15] PAPy was prepared by a chemical oxidative procedure with $FeCl_3$ as an oxidant [Fig. 1(b)]. APy (0.01 mol) was added dropwise to 60 mL of a stirred chloroform ($CHCl_3$) solution with $FeCl_3$ (0.03 mol) in a nitrogen atmosphere. The mixture was stirred at room temperature for 8 h, and then, methanol (100 mL) was added to the flask to terminate the polymerization.

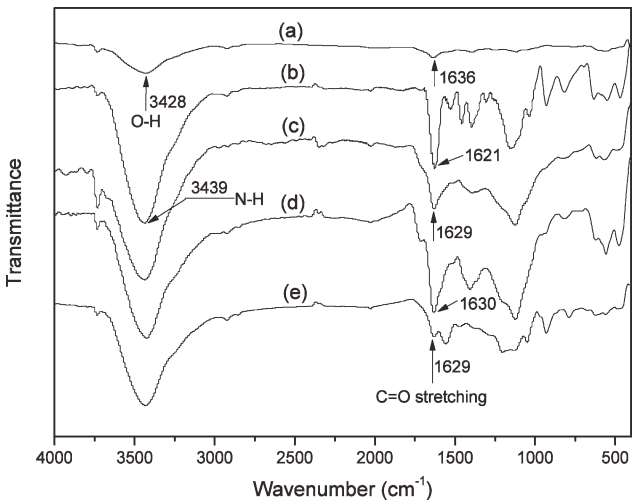

Figure 2 FTIR spectra of the MWNTs, PAPy, and PAPy (or PPy)/MWNT composites: (a) MWNTs, (b) PAPy, (c) APy/MWNTs = 2.5:1, (d) APy/MWNTs = 5:1, and (e) Py/MWNTs = 2.5:1.

The product was filtered and washed with copious amounts of methanol until the solution became colorless. The resulting powder was dried *in vacuo* at 60°C for 24 h.

PAPy/MWNT composites were prepared by the *in situ* chemical polymerization of APy on MWNTs [Fig. 1(c)]. The MWNTs (0.2 g) were first dispersed in a mixed solvent of $CHCl_3$ and acetonitrile solution by sonication in a nitrogen atmosphere at room temperature for 2 h with a bath sonicator. Thereafter, 20 mL of $CHCl_3$/acetonitrile solution with APy (0.5 g) was added to the suspension with further sonication for 1 h. $FeCl_3$ solution (20 mL) was slowly added to this solution with constant sonication. The reaction mixture was again sonicated at ambient temperature for 4 h. The Fe^{3+}/APy molar ratio was 3. Finally, the mixture was purified as described previously for PAPy (filtering, multiple washings, decanting, and vacuum drying). The feeding mass ratios of the APy and MWNTs were 2.5:1 (APy/MWNTs = 0.5:0.2) and 5:1 (APy/MWNTs = 1.0:0.2), respectively. As a comparison, the PPy/MWNT composites were fabricated by a similar procedure to produce PAPy/MWNT composites. The feeding mass ratio of the Py and MWNTs was 2.5:1 (Py/MWNTs = 0.5:0.2).

Characterization of the composites

Fourier transform infrared (FTIR) spectra were recorded on a Nicolet 5700 spectrometer (Wisconsin, USA), and samples were run as pressed KBr pellets. X-ray diffraction (XRD) was studied in the 2θ range of 5–60° with a Rigaku D/max Ultima III X-ray diffractometer (Tokyo, Japan) with Cu Kα targets at a scan rate of 4°/min. The surface morphology of some selected samples was observed with a field emission scanning electron microscope (FE-SEM; Nova NanoSEM 230, FEI). Transmission electron microscopy (TEM) images of the samples were obtained with a Tecnai G2 F20 S-TWIN 200-kV transmission electron microscope (FEI). Thermogravimetric analysis (STA449C, Netzsch) was carried out in a nitrogen atmosphere with a heating rate of 10°C/min within the temperature range from room temperature to 800°C.

A powder sample of 0.1 g was loaded and pressed into a pellet 13 mm in diameter with the help of a hydraulic pressure instrument (Tianjin Keqi High and New Technology Corporation, Tianjin, China) at 10 MPa of pressure for 2 min, and the thickness of each pellet was measured by a Vernier caliper (Shanghai, China). Then, the room-temperature electrical conductivity of the pellets was measured by a standard four-probe method with an SDY-4 four-point probe meter.

RESULTS AND DISCUSSION

The FTIR spectra of the MWNTs, PAPy, and PAPy (or PPy)/MWNT composites are shown in Figure 2. The presence of polar functional groups in the samples was confirmed by FTIR spectra. The characteristic bands at 3428, 1636, and 1118 cm^{-1} were assigned to the O—H stretching, C=O stretching, and C—C—O stretching vibrations, respectively, in the MWNTs. For PAPy, a strong broad absorption band around 3439 cm^{-1} corresponded to the N—H stretching, and a strong characteristic band at 1621 cm^{-1} was consistent with the C=O stretching vibration. The band of the Py-ring fundamental vibration appeared at 1520 cm^{-1}, and the C—H in-plane

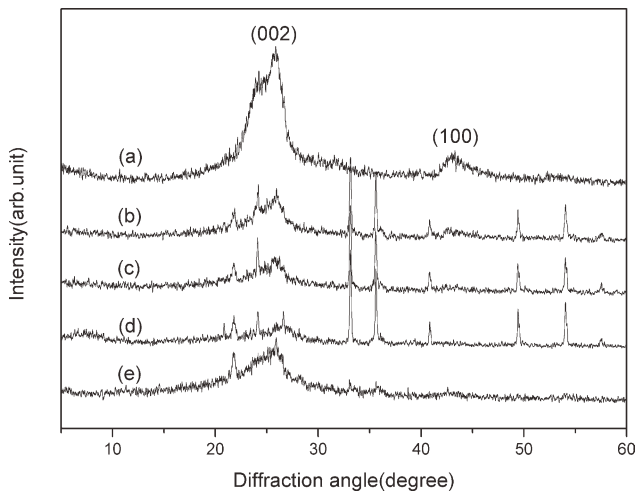

Figure 3 XRD patterns of the PAPy, MWNTs, and PAPy (or PPy)/MWNT composites: (a) MWNT, (b) APy/MWNTs = 2.5:1, (c) APy/MWNTs = 5:1, (d) PAPy, and (e) Py/MWNTs = 2.5:1.

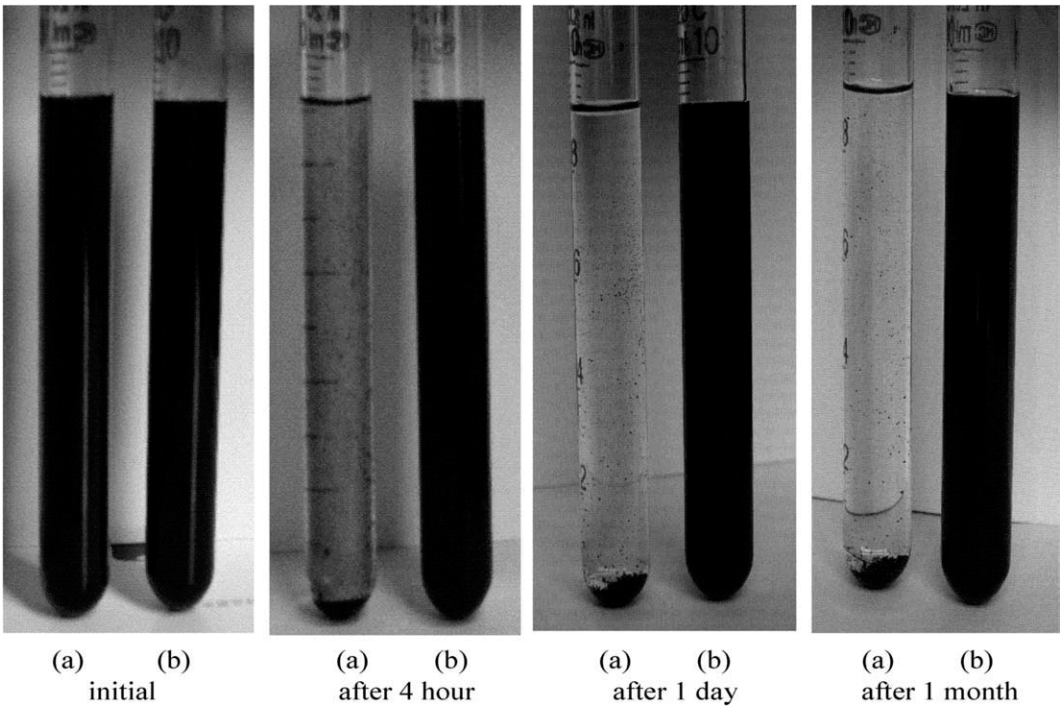

Figure 4 Photographs of the solution stability of the suspension with composites in ethanol solution: (a) PPy/MWNTs (Py/MWNTs = 2.5:1) and (b) PAPy/MWNTs (APy/MWNTs = 2.5:1).

deformation vibration and C—N stretching vibration appeared at 1039 and 1141 cm^{-1}, respectively. The C—H stretching vibration bands of the methyl group (CH_3) were observed around 2921 and 2854 cm^{-1}. The PAPy/MWNT composites showed characteristics bands of both MWNTs and PAPy. However, it

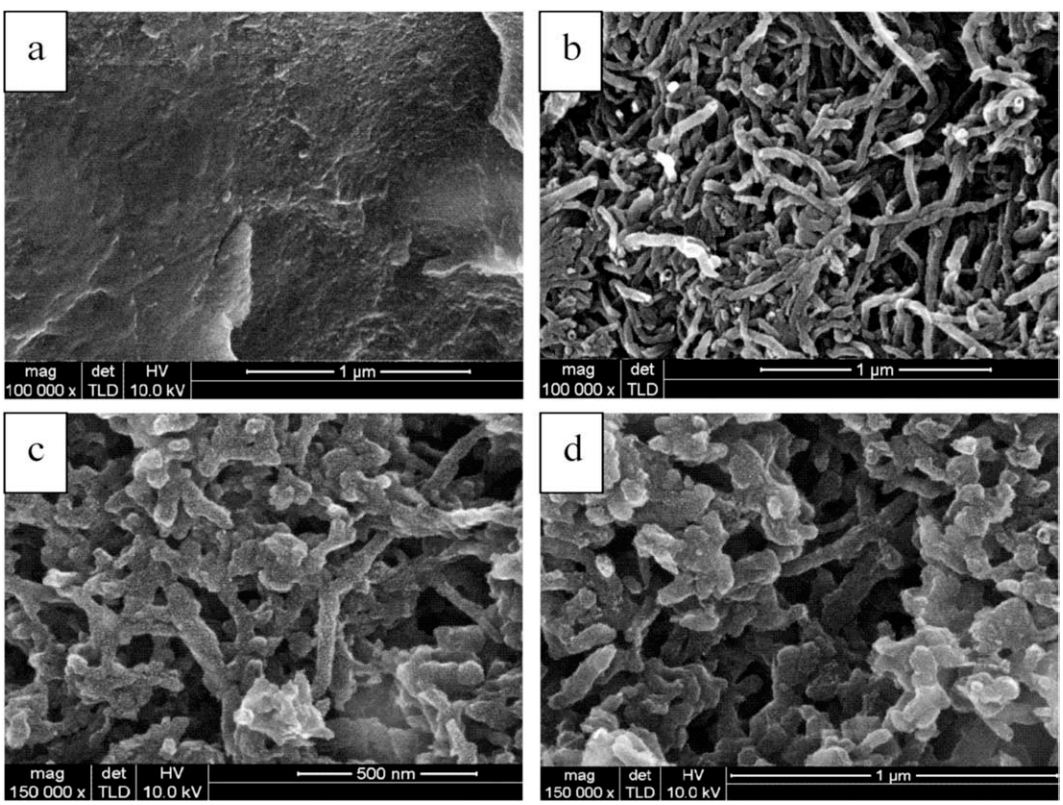

Figure 5 FE-SEM images of the PAPy, MWNTs, and PAPy/MWNT composites: (a) PAPy, (b) MWNTs, (c)APy/MWNTs = 2.5:1, and (d) APy/MWNTs = 5:1.

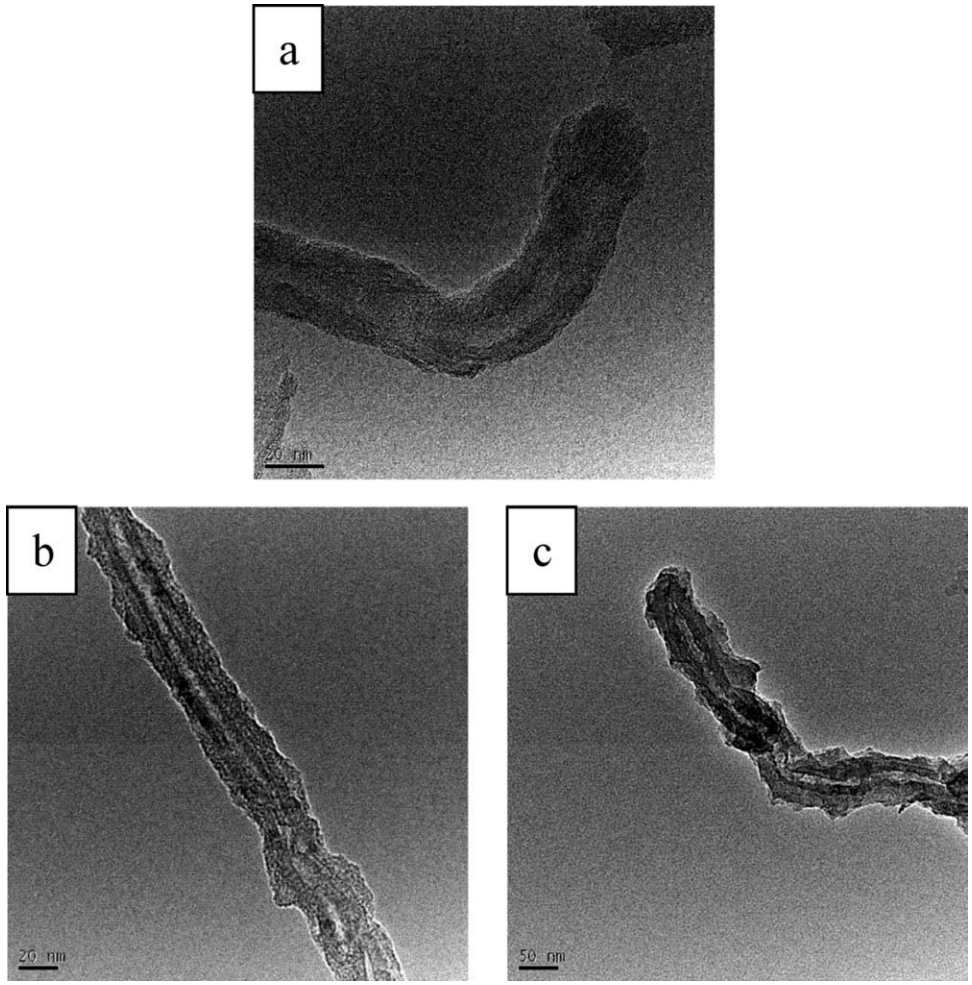

Figure 6 TEM images of MWNTs and PAPy/MWNT composites: (a) MWNTs, (b) APy/MWNTs = 2.5:1, and (c) APy/MWNTs = 5:1.

was clear that the band of C=O groups shifted from 1636 cm^{-1} in the MWNTs and 1621 cm^{-1} in PAPy to 1629 cm^{-1} in the PAPy/MWNT composites. As a comparison, the FTIR spectrum of the PPy/MWNT composites is also shown in Figure 2(e). The composites, because of the PPy without the C=O groups, only showed a low-intensity peak of C=O groups for the MWNTs compared to the PAPy/MWNT composites. Furthermore, no additional peaks were observed in the FTIR spectra of the PAPy (or PPy)/MWNT composites, except for the characteristic peaks of PAPy (or PPy) and the MWNTs. Therefore, no chemical reaction occurred between the PAPy (or PPy) and the MWNTs.

XRD patterns of the PAPy, MWNTs, and PAPy (or PPy)/MWNT composites are presented in Figure 3. The XRD pattern of the MWNTs indicated the presence of two diffraction peaks at $2\theta = 25.82°$ ($d = 3.45$ Å) and 43.10° [$d = 2.10$ Å; Fig. 3(a)] corresponding to the (002) and (100) reflections, respectively, of the carbon atoms; this was in good agreement with the literature.[16] The Bragg diffraction peaks at $2\theta =$ 20.83, 21.89, 24.07, 26.63, 33.13, 35.58, 40.83, 49.44, 54.04, and 57.57° [Fig. 3(d)] suggested a well-crystallized pure PAPy. For the PAPy/MWNT composites, the XRD patterns exhibited both characteristic PAPy multipeaks and broad MWNTs peaks. From Figure 3(b,c), it was clear that the intensity of the peaks around 25.8 and 43.1° decreased with increasing mass ratio of APy to MWNTs. However, the intensity of peaks at about 33.1, 35.6, 40.8, 49.4, 54.0, and 57.6° increased with increasing mass ratio of APy to the MWNTs. The XRD pattern of the PPy/MWNT composites is also shown in Figure 3(e), and the pattern was quite different from PAPy/MWNT composites because of the completely amorphous structure of PPy.

It is known that modified CNTs can be completely dispersed by sonication in some polar solutions, such as water and ethanol. However, PPy is completely insoluble in any solvent, either polar or nonpolar. Photographs of the solution stability of the suspension with the composites in ethanol solution are shown in Figure 4. After 4 h, the deposition of the PPy/MWNT composites [Fig. 4(a)] clearly

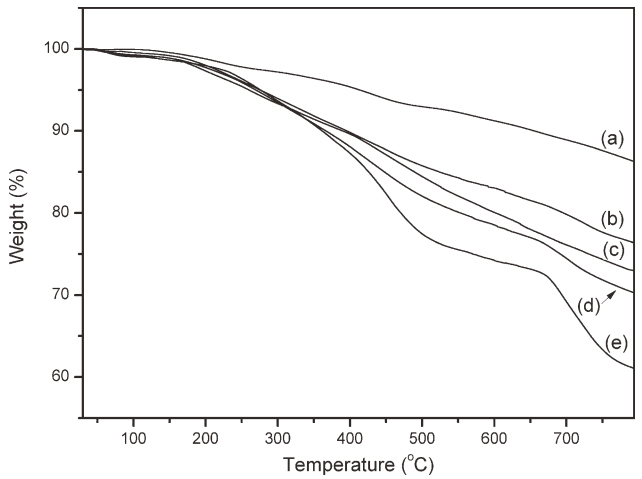

Figure 7 Thermogravimetric curves of the PAPy, MWNTs, and PAPy (or PPy)/MWNT composites: (a) MWNTs, (b) APy/MWNTs = 2.5:1, (c) Py/MWNTs = 2.5:1, (d) APy/MWNTs = 5:1, and (e) PAPy.

indicated that the MWNTs were successfully coated with PPy. In the case of the PAPy/MWNT composites, most of the composites remained suspended for over a month because they were dispersed [Fig. 4(b)]. This was because PAPy, with polar acetyl substituents, increased the dispersion of the composites in some polar solvents. (The external surface of the composites was PAPy or PPy, as shown in Figs. 5 and 6.) The real interaction of the composites and solvent was that of PAPy (or PPy) and the solvent. So, the interaction of PAPy with polar substituents (acetyl) and solvent enhanced the dispersion of PAPy in some polar solvents compared to unsubstituted PPy.

Figure 5 shows the FE-SEM images of the PAPy, MWNTs, and PAPy/MWNT composites. A typical morphology of PPy was reported earlier.[13] The particle size of PPy was 200–400 nm with a spherical morphology. However, the image of PAPy was a block; we found no spherically shaped particles, and the surface of the sample was smooth [Fig. 5(a)] because of the crystallization of PAPy, which was consistent with the results of XRD. For the MWNTs, many nanotubes were entangled together without any impurities on their surface, as shown in Figure 5(b). The scanning electron microscopy images of the PAPy/MWNT composites are presented in Figure 5(c,d). It was clear that the surface of the CNTs was quite uniformly coated with PAPy, and the diameter of the PAPy/MWNTs increased from 10 to 30 nm for the MWNTs to 30–50 nm for the PAPy/MWNTs (2.5:1) and 40–70 nm for the PAPy/MWNTs (5:1). Furthermore, their external surface was less smooth.

The tubular morphology of the MWNTs and PAPy/MWNT composites was also imaged by TEM, as presented in Figure 6. The TEM images of the MWNTs and PAPy/MWNT composites revealed that both the MWNTs and PAPy/MWNT composites were hollow, and PAPy was only coated on the surface of the CNTs. As shown in Figure 6(b,c), the thickness of the PAPy coating on each nanotube was observed to increase and was dependent on the ratio of the APy and MWNTs.

Figure 7 reveals the thermogravimetric analysis thermograms of the MWNTs, PAPy, and PAPy/MWNT composites. The MWNTs were quite stable and showed a small decomposition in the temperature range 20–800°C, and a total mass loss of about 14% at 800°C was observed because of a small amount of water or the presence of functional groups [Fig. 7(a)]. Pure PAPy did not reveal any obvious weight loss below 220°C and showed only a 2% mass loss. A rapid mass loss, however, occurred in the ranges 220–500 and 670–800°C, and 61% of the mass was preserved at 800°C. The PAPy/MWNT composites displayed more delayed decomposition compared to pure PAPy, and more mass remained at 800°C. The thermal stability of the PAPy/MWNT composites increased with decreasing mass ratio of the APy and MWNTs, which indicated that the CNTs were able to improve the thermal stability of the PAPy/MWNT composites. The total mass losses up to 800°C were estimated to be about 14, 23, 27, 30, and 39% for the MWNTs, PAPy/MWNT composites (APy/MWNTs = 2.5:1), PPy/MWNT composites (Py/MWNTs = 2.5:1), PAPy/MWNT composites (APy/MWNTs = 5:1), and PAPy, respectively. Here, the trend of the degradation curves of the PAPy/MWNT composites was similar to that of PAPy, and the degradation of the PAPy/MWNT composites was mainly dominated by PAPy.

Finally, the room-temperature electrical conductivity of the MWNTs, PAPy, and PAPy (or PPy)/MWNT composites was measured by a standard four-probe method, as shown in Table I. The electrical conductivity of the MWNTs and PAPy were 1.67 and 9.0×10^{-4} S/cm, respectively. The conductivity of the PAPy/MWNT composites (1.25 S/cm for APy/MWNTs = 2.5:1 and 0.15 S/cm for APy/

TABLE I
Room-Temperature Conductivity of the MWNTs, PAPy, and PAPy (or PPy)/MWNT Composites

Sample	MWNTs	PAPy	PAPy/MWNTs (APy/MWNTs = 2.5:1)	PAPy/MWNTs (APy/MWNTs = 5:1)	PPy/MWNTs (Py/MWNTs = 2.5:1)
Conductivity (S/cm)	1.67	9.0×10^{-4}	1.25	0.15	0.91

MWNTs = 5:1) was remarkably higher than that of PAPy but lower than that of the MWNTs. On the basis of the data of the conductivities (Table I), the enhanced conductivity of the composites was mainly attributed to the CNTs. Because of their large surface area and aspect ratio, the MWNTs may have served as a conducting bridge, connecting PAPy conducting domains and increasing the effective percolation.[13,17] Furthermore, it was found that the electrical conductivity of the PAPy/MWNT composites was reduced with increasing mass ratio of APy to the MWNTs.

CONCLUSIONS

PAPy/MWNT composites were prepared via *in situ* chemical polymerization. The FTIR results indicate that no chemical reaction occurred between the PAPy and MWNTs, and only the MWNTs served as a template for APy polymerization. The solution stability of the suspension with the PAPy (or PPy)/MWNT composites was investigated, and the results show that the PAPy/MWNT composites had an excellent dispersion in some solvents compared to the PPy/MWNT composites. The thickness of the PAPy coating on each nanotube, the electrical conductivity, and the thermal stability of the PAPy/MWNT composites were dependent on the ratio of PAPy to the MWNTs. The resulting composites could be used for the development of new applications in electrode materials and other fields.

References

1. Treacy, M. M.; Ebbesen, T. W.; Gibson, T. M. Nature 1996, 381, 678.
2. Ago, H.; Kugler, T.; Cacialli, F.; Petritsch, K.; Friend, R. H.; Salaneck, W. R.; Ono, Y.; Yamabe, T.; Tanaka, K. Synth Met 1999, 103, 2494.
3. Ajayan, P. M. Chem Rev 1999, 99, 1787.
4. Baughman, R. H.; Zakhidov, A. A.; De, H.; Wait, A. Science 2002, 297, 787.
5. Zanello, L. P.; Zhao, B.; Hu, H.; Haddon, R. C. Nano-Lett 2006, 6, 562.
6. Gruner, G. J Mater Chem 2006, 16, 3533.
7. Lee, K.; Cho, S.; Park, S. H.; Heeger, A. J.; Lee, C. W.; Lee, S. H. Nature 2006, 41, 65.
8. Dallas, P.; Stamopoulos, D.; Boukos, N.; Tzitzios, V.; Niarchos, D.; Petridis, D. Polymer 2007, 48, 3162.
9. Jin, G.; Norrish, J.; Too, C.; Wallace, G. Curr Appl Phys 2004, 4, 366.
10. Georgakilas, V.; Dallas, P.; Niarchos, D.; Boukos, N.; Trapalis, C. Synth Met 2009, 159, 632.
11. Groenendaal, L.; Jonas, F.; Freitag, D.; Pielartzik, H.; Reynolds, J. R. Adv Mater 2000, 12, 481.
12. Han, G.; Yuan, J.; Shi, G.; Wei, F. Thin Solid Films 2005, 474, 64.
13. Sahoo, N. G.; Jung, Y. C.; So, H. H.; Cho, J. W. Synth Met 2007, 157, 374.
14. Karim, M. R.; Lee, C. J.; Chowdhury, A. M. S.; Nahar, N.; Lee, M. S. Mater Lett 2007, 61, 1688.
15. Zhang, Z. G.; Wu, H. C.; Zhang, Z. F.; Yi, W. H. Fine Chem 2004, 21, 324.
16. Endo, M.; Takeuchi, K.; Hiroka, T.; Furuta, T.; Kasai, T.; Sun, X.; Kiang, C. H.; Dresselhaus, M. S. J Phys Chem Solids 1997, 58, 1707.
17. Zengin, H.; Zhou, W.; Jin, J.; Czerw, R.; Smith, D. W., Jr.; Echegoyen, L.; Carroll, D. L.; Foulge, S. H.; Ballato, J. Adv Mater 2002, 14, 1480.